



HAL
open science

An improved combination of tensile strength and ductility in titanium alloys via oxygen ordering

Fabienne Amann, Régis Poulain, Stéphanie Delannoy, Jean-Philippe Couzinié,
Emmanuel Clouet, Ivan Guillot, Frédéric Prima

► **To cite this version:**

Fabienne Amann, Régis Poulain, Stéphanie Delannoy, Jean-Philippe Couzinié, Emmanuel Clouet, et al.. An improved combination of tensile strength and ductility in titanium alloys via oxygen ordering. *Materials Science and Engineering: A*, 2023, 867, pp.144720. 10.1016/j.msea.2023.144720 . cea-03972983

HAL Id: cea-03972983

<https://cea.hal.science/cea-03972983>

Submitted on 3 Feb 2023

HAL is a multi-disciplinary open access archive for the deposit and dissemination of scientific research documents, whether they are published or not. The documents may come from teaching and research institutions in France or abroad, or from public or private research centers.

L'archive ouverte pluridisciplinaire **HAL**, est destinée au dépôt et à la diffusion de documents scientifiques de niveau recherche, publiés ou non, émanant des établissements d'enseignement et de recherche français ou étrangers, des laboratoires publics ou privés.

An improved combination of tensile strength and ductility in titanium alloys via oxygen ordering

F. Amann^{1,2}, R. Poulain^{1,2,3}, S. Delannoy^{1,3}, J. P. Couzinié², E. Clouet⁴, I. Guillot², F. Prima¹

¹ Université PSL, Chimie ParisTech–CNRS, Institut de recherche de Chimie Paris (UMR 8247), F-75005 Paris, France

² Univ Paris Est Creteil, CNRS, ICMPE, UMR 7182, 2 rue Henri Dunant, 94320 Thiais, France

³ Biotech Dental SAS, 305 allées de Craonne, F-13300 Salon-de-Provence, France

⁴ Université Paris-Saclay, CEA, Service de Recherches de Métallurgie Physique, F-91191 Gif-sur-Yvette, France

Abstract

Oxygen content has always been limited in commercial titanium and titanium alloys due to its propensity to induce a severe ductility loss. Yet, its effect on the macroscopical behavior has never been clearly understood and is still rather unclear considering the wide variability in the literature results. Here, we investigate the tensile properties of α -titanium with oxygen contents ranging from 0.15 to 0.80 weight percent (wt%). While the strain-hardening ability of oxygen is maintained, no ductility drop is observed up to 0.60wt% of oxygen, thus allowing exceptional combinations of mechanical properties with an ultimate tensile strength (UTS) of 800 MPa and 29% of elongation at fracture for the Ti-0.6O alloy. Both high strength and ductility of these alloys result from the dislocations/precipitate's interactions. It is proposed that these interactions induce an important cross-slip activity responsible for a dislocation multiplication and a high work-hardening rate. With the addition of Zr, alloys exhibit an even more promising combination of mechanical properties, achieving 1,075MPa of UTS and 28% of elongation at fracture for the Ti-4.5Zr-0.8O alloy. The mechanical properties of TiO and TiZrO alloys brought out in this study surpass those of Ti-6Al-4V

alloy and open significant prospects for developing a new generation of oxygen-tolerant titanium alloys.

Keywords

Titanium alloys, Mechanical properties, Oxygen strengthening, Electron microscopy

1. Introduction

Titanium and titanium alloys are mostly used for mechanically-demanding applications, such as biomedical or aerospace [1], where in-service material's durability, including at high temperature [2], is safety critical. The main factor prohibiting a wider use of titanium lies in its cost [3], which especially arises from the technical measures put in place to prevent oxygen contamination during fabrication and thermomechanical processes [4].

For the last seventy years, oxygen addition has been reported to induce a dramatic drop in elongation-to-failure in α -titanium [5–10], which explains the limitation of its content below 0.4wt% in commercially pure titanium grades [11,12] and the necessity to set up strategies for avoiding oxygen contamination during industrial processes. Further analysis of existing data, though, leads to a more ambivalent outcome, due to a high variability in the measured elongation-to-failure [8,10,13], and also because some recent works do not evidence any elongation-to-failure loss with oxygen addition [14–16]. In some Ti- β alloys, such as TNTZ, oxygen is already known to induce a particular mechanical behavior coupling a strong strengthening and a maintenance of a high level of elongation-to-failure [17].

There is thus a major interest in understanding the impact of oxygen on the mechanical properties of α -titanium, since the development of oxygen-tolerant α -

titanium alloys may lead up to cost-saving evolutions in the titanium industry. This is even more crucial considering the substantial strengthening effect of oxygen in titanium alloys, even at low concentration [10,13,16].

Until very recently, our understanding of the oxygen impact relied solely on a picture where randomly distributed oxygen atoms in solid solution interact with gliding dislocations and lead to an intense hardening [8,18–21]. This view was precisely challenged by a recent work highlighting the presence of Ti_6O -type oxygen-ordered nanoprecipitates in titanium [22], suggesting that a paradigm shift is required to fully grasp the complex contributions of oxygen in titanium.

This work aims to demonstrate that binary Ti-O alloys do not systematically suffer from an elongation-to-failure decrease. For this purpose, titanium alloys with varying oxygen contents ranging from 0.15 to 0.80wt% were prepared and their mechanical properties were investigated using tensile tests. The results were then discussed regarding the influence of the Ti_6O -type precipitates on the deformation mechanisms. Finally, as a first valorisation of these results, the latter were extrapolated to ternary Ti-Zr-O alloys, in which zirconium brings supplementary strengthening contributions [23].

2. Materials and method

Titanium and zirconium sponges with high purity (99.9%) were used to prepare 200g arc-melted ingots of Ti-O and Ti-Zr-O alloys. The addition of TiO_2 powder allowed to accurately control the oxygen content. The ingots were then hot rolled around 1,173K into square bars and heated at 923K during 1.8ks for complete recrystallization. At this step, the chemical composition of each alloy was measured by inert gas fusion analysis for oxygen and nitrogen and by Inductively Coupled Plasma - Optical Emission

Spectrometry (ICP-OES) for zirconium (Table 1). Slices were cut and subsequently hot and cold rolled with thickness reductions of 75% and 40%, respectively, for each step, leading to 0.6mm plates. The latter were finally recrystallized at 1,023K for 600s in molten salts baths (Li_2CO_3 , Na_2CO_3 , K_2CO_3) and water quenched.

Nominal compositions	Oxygen (wt%)	Nitrogen (wt%)	Zirconium (wt%)
Ti-0.15	0.157	< 0.020	-
Ti-0.40	0.392	0.007	-
Ti-0.60	0.643	0.006	-
Ti-0.80	0.768	0.028	-
Ti-4.5Zr-0.15O	0.147	0.004	4.50
Ti-4.5Zr-0.40	0.374	0.010	4.46
Ti-4.5Zr-0.60	0.561	0.003	4.46
Ti-4.5Zr-0.80	0.835	0.003	4.42

Table 1 : Chemical compositions of the alloys obtained by gas fusion analysis for oxygen and nitrogen and by Inductif Coupled Plasma – Optical Emission Spectrometry for zirconium

After manual polishing with SiC grinding papers, samples were electropolished with a Struers LectroPol-5 machine using an electrolyte solution composed of perchloric acid (6%), hydrochloric acid (4%), 2-butoxyethanol (34%) and methanol. Grain size and crystallographic orientations were analyzed by Electron Backscatter Diffraction (EBSD) using a LEO 1530 SEM. Maps were obtained with a 20kV voltage and a step size of 0.6 μm . The grain size was determined by the mean circle diameter of the detected grains with a misorientation threshold of 5° with the OIM software [24].

Flat dog-bone specimens of 0.6mm thickness and 20mm gauge length were machined along the rolling direction for tensile tests. For each composition, two reproducible tests were performed at room temperature (RT) on a 10kN INSTRON 5966 electro-mechanical machine. A 10mm gauge length extensometer was used, and a fixed strain-rate of 10^{-3}s^{-1} was imposed. The true plastic deformation $\epsilon_{p,true}$ and true stress

σ_{true} are calculated with the data from tensile tests. The work-hardening rate $\theta = \delta\sigma_{\text{true}}/\delta\varepsilon_{\text{p,true}}$ was computed according to the plastic true strain. The Considere criterium was used to suspend the curves when $\theta = \sigma_{\text{true}}$.

Transmission Electron Microscopy (TEM) observations were performed on both undeformed and 1%-strained samples. For this purpose, 3mm discs were cut and mechanically polished to a thickness of 100 μm using SiC grinding papers. They were then electrolytically thinned using a twin jet Struers Tenupol apparatus with a solution of butanol (27%), perchloric acid (7%) and methanol at a voltage of 25V. A low temperature between 253 and 263K is used to prevent the formation of hydrides. Images of ordered precipitates and corresponding diffraction patterns were obtained with a JEOL 2100+ electron microscope working at 200kV. The Scanning-TEM (STEM) images in Ti-O were captured with a FEG-equipped Tecnai F20 in the Annular Bright Field (ABF) image mode.

3. Results and discussion

The microstructure of the Ti-xO samples presents equiaxed α -grains with a (0001) texture and the basal plane parallel to the normal direction (fig. 1). This texture is typical for a fully-recrystallized α -titanium alloy [25]. The grain size tends to decrease when the oxygen content increases from 45 μm at 0.15wt% to 19 μm at 0.80wt% (fig. 1.e). This point can be ascribed to an oxygen-induced solute drag effect that limits grain growth during thermal annealing [26]. At a finer scale, nanometric precipitates whose size is in the 15-30nm range are observed by TEM in dark-field conditions (fig. 1.f). The diffraction signature of these precipitates is highlighted by a red circle in figure 1.g. It was previously shown that they actually display a Ti_6O -type crystal structure coming

from an oxygen ordering mechanism in the octahedral interstitial sites of the hexagonal close-packed lattice [22].

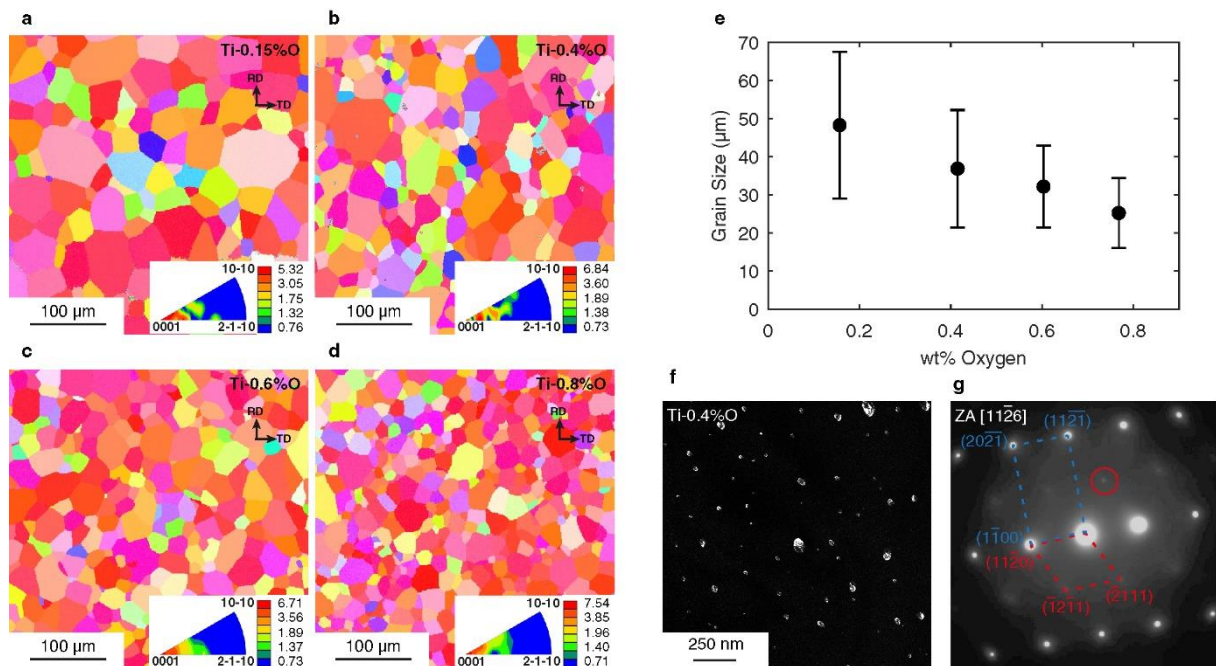


Fig. 1. Left side: EBSD normal direction Inverse Pole Figure (IPF) orientation maps of the Ti-xO alloys and corresponding inverse pole figures for the direction (0001), with $x = 0.15$ (a), 0.40 (b), 0.60 (c) and 0.80 (d) wt%. RD and TD correspond to the rolling and transverse directions, respectively. Right side: Evolution of the average grain size according to oxygen content (e). Dark-field TEM image of the Ti₆O precipitates in Ti-0.4O (f) and corresponding Selected Area Diffraction Pattern (SADP) (g). The spots indexed in blue correspond to matrix reflections in the matrix zone axis [1126] and the spots indexed in red to precipitates reflections in the precipitate zone axis [1103]. The red circle shows which reflection has been used to record the precipitates.

The figure 2.a shows the engineering strain-stress curves of the Ti-O alloys strained at RT. Below 0.6wt%, the Yield Strength (YS) increases linearly with the oxygen content, by 75 MPa per 0.1wt%O, from 400 to 700MPa. As reflected in figure 2.b, this evolution is consistent with previous studies [6-7-9-10-14]. While this evolution remains linear above 0.6wt% in the literature, a slope-break is observed at 0.8wt% of oxygen in our study. At this content, the values of YS and UTS reach respectively 1,190 and 1,220MPa, then suggesting a change of behavior for O content between 0.6 and 0.8wt%.

This level of oxygen also seems to be a turning point regarding the elongation-to-failure. Indeed, while most of literature results followed a linear trend, showing a gradual and significant decrease in elongation at fracture with the oxygen addition, this work surprisingly highlights the maintenance of a high level of elongation-to-failure (around 30%) up to 0.6wt% and then a sharp fall above this value, to decline to less than 10%.

Even if the remarkable maintaining of the elongation-to-failure up to oxygen contents as high as 0.6wt% contrasts with several reports, this was nevertheless already observed in the work of Sun *et al.* [14]. Interestingly, the XRD diffractograms depicted in this article systematically displayed shoulders on the left side of each α -phase peak. These shoulders have proved to be consistent with the Ti_6O structure [21], thus suggesting that, in both works, Ti_6O -type precipitates are present. These precipitates may hence play a key role in maintaining elongation-to-failure despite high amounts of oxygen.

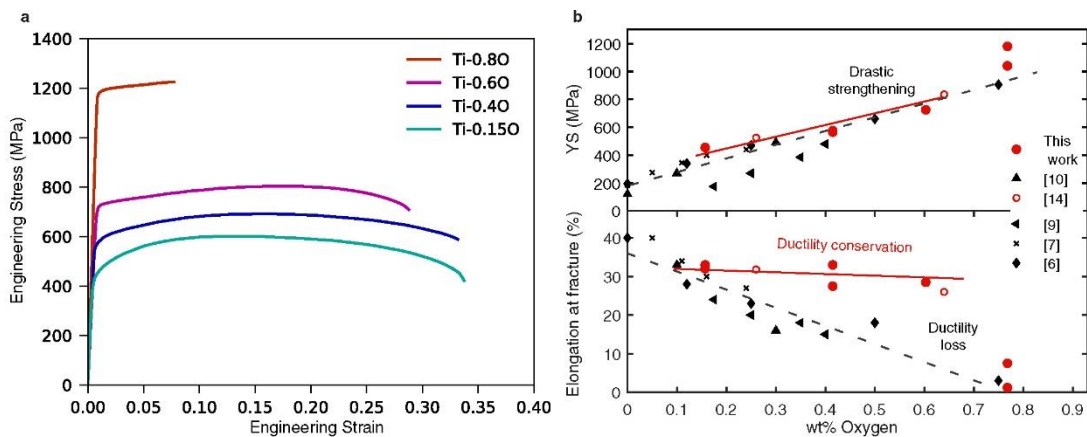


Fig. 2. Engineering stress-strain curves of the Ti-xO alloys (a). Comparison of the mechanical properties, yield stress and elongation at fracture, of the Ti-xO alloys of the present studies with previous works also in binary Ti-O alloys (b).

Observations in the 1%-strained Ti-0.40 sample in STEM mode gives an overview of the dislocations network. Dislocations appearing wavy and the presence of multiple pinning points (fig. 3.a and 3.b) suggest a strong interaction between the dislocations

and the precipitates. This may mean that the hardening effect due to the presence of oxygen in binary Ti-O alloys cannot be attributed solely to the solid solution effect, and that the additional presence of ordered nanoprecipitates also seems to make a significant contribution to the increase of the strength of the alloys.

STEM micrographs also exhibit slip bands in which dislocations are confined (fig. 3.c), suggesting a localization of plastic deformation in these alloys at the microscale. This can be reasonably explained by a shearing mechanism of the nanoprecipitates, eased by their small size and small parametric mismatch with the matrix [21]: a first dislocation shears the precipitates and opens a way for following dislocations that can glide in the same direction [10,27]. Moreover, the loops and debris present in these slip bands may result from a profuse cross-slip activity due to the strong interaction between the precipitates and the dislocations [18,20,21,28] (fig. 3.c). The phenomena observed here, namely the localization of plastic deformation associated with an important cross-slip activity within the bands, underlines the possibility for dislocations to strongly interact with each other, leading to forest hardening. This effect is macroscopically studied by looking at the evolution of the work-hardening rate plotted as a function of the true plastic strain.

In figure 3.d, clear changes in work-hardening rate can be observed depending on oxygen content. At low concentrations (0.15wt%), the work-hardening rate is high at early deformation stage and then rapidly decreases. For oxygen content above 0.4wt%, the work-hardening rate sharply decreases up to 0.01 of plastic true strain and a plateau is then reached. A nearly perfect elastoplastic transition is even observed for the Ti-0.6O and Ti-0.8O alloys. These behaviors are in contrast with previous studies on titanium such as, for example, the work of Chong *et al.*, where the work-hardening rate drastically decreases with oxygen addition and becomes negative for a

deformation as low as 0.05 in titanium with only 0.3wt% of oxygen, at same strain-rate and temperature [10]. In this previous study, it is suggested that the loss of ductility arises from the strong decrease in “strain hardening ability”. In our work, the combined effect of an increase in work-hardening with oxygen content and the high value of such work-hardening, even at an advanced deformation stage, could explain the possibility for the material to reach large deformation before necking and thus the high elongation at fracture finally obtained.

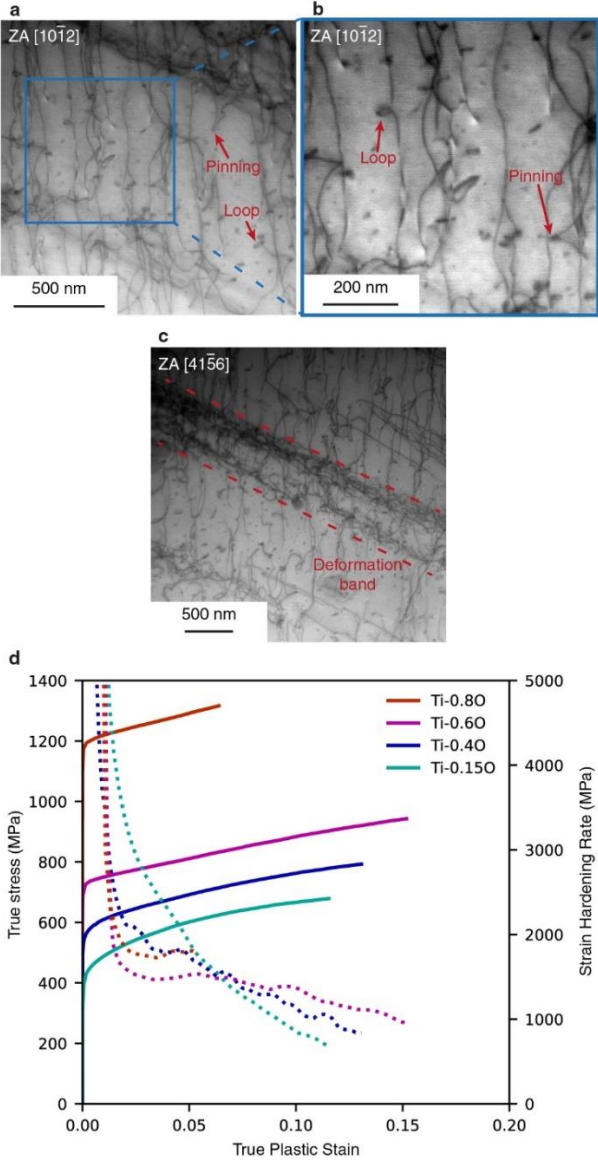


Fig. 3. Large-scale STEM (a and c) and lower-scale (b) STEM images taken in Ti-0.4O alloy deformed at 1% plastic strain in ABF conditions. The Zone Axes (ZA) of the different TEM images are indicated on each picture. True stress – true plastic strain curves of Ti-xO alloys (solid lines) and corresponding work-hardening rates (dotted lines) (d).

4. Extrapolation to a ternary Ti-Zr-O system

The results mentioned above open new perspectives for the development of oxygen-tolerant and -strengthened titanium alloys. On this basis, Ti-4.5Zr-xO alloys with x ranging from 0.15 to 0.80wt% were prepared to assess if oxygen tolerance tendency observed in binary Ti-O alloys could be improved by the addition of a second alloying element. Zirconium is specifically chosen here since it is a neutral element, i.e. neither α - nor β -stabilizer [29], chemically close to titanium and completely miscible with titanium [30]. These properties allow to keep a similar α -phase microstructure with a substitutional alloying element providing a significant strengthening effect both through solid solution effect and grain refinement [31]. Moreover, the biocompatibility of both zirconium and titanium allows these alloys to be used for biomedical applications [32]. The amount of 4.5wt% of zirconium is chosen as it is necessary and sufficient to significantly decrease the grain size [31]. The Ti-4.5Zr-xO alloys present the same microstructure as in Ti-xO alloys, with Ti_6O -type precipitates but finer grains (see Supplementary Figure 1), and similar dislocation networks with deformation bands (see Supplementary Figure 2). Nevertheless, the present section only focuses on the mechanical properties.

The engineering stress-strain curves of the Ti-4.5Zr-xO alloys are gathered in figure 4.a. As observed previously in Ti-O alloys, the YS increases linearly at a similar rate with oxygen addition, but no discontinuity is observed in the evolution, even for the addition of 0.8wt%-O (fig. 4.b). For a same oxygen content, the increase in YS in the Ti-Zr-O alloys family compared to the binary system can be attributed to an additional

solid solution strengthening and a Hall-Petch mechanism due to the addition of zirconium.

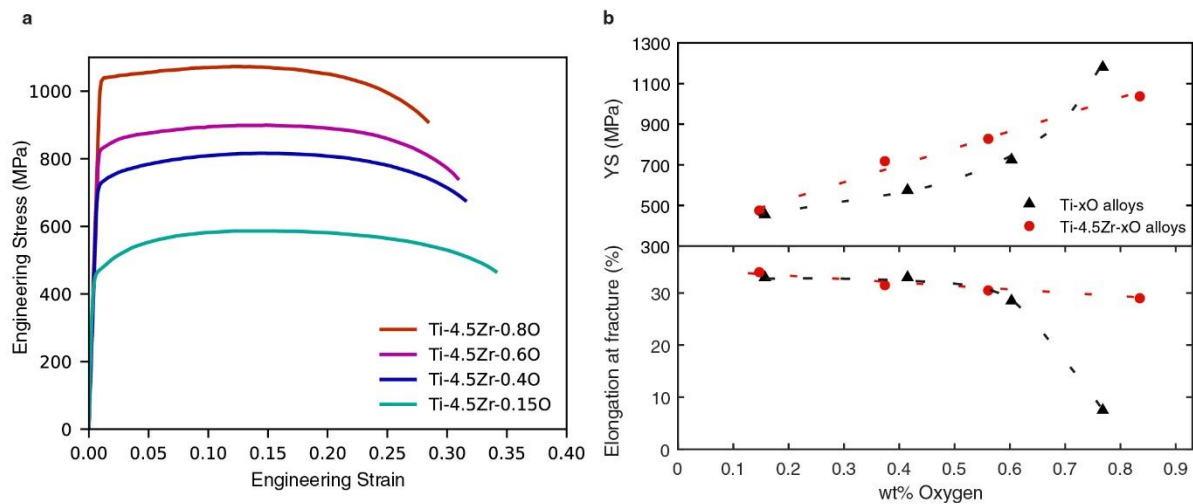


Fig. 4. Engineering stress-strain curves of the Ti-4.5Zr-xO alloys (a) and comparison of the mechanical properties, yield stress and elongation at fracture, of the Ti-4.5Zr-xO with Ti-xO alloys (b). The dashed lines are plotted to facilitate the lecture.

As depicted in figure 4.b, all the prepared Ti-4.5Zr-xO alloys keep a high level of ductility (close to 30% at fracture). For the highest oxygen content (0.8wt%), the elongation at fracture is still extremely high, thus offering an exceptional combination of resistance and ductility (UTS of 1,075MPa and 28% of elongation at fracture), which has rarely been reached in any other titanium alloys [33,34]. As for the rupture mechanisms, a comparison of both alloy families shows a mixed fracture surface with dimples and intergranular decohesion (see Supplementary Figure 3) suggesting a rather ductile fracture. As a result, both Ti-O and Ti-Zr-O alloys families are shown to overcome the strength/ductility trade-off and fill in an empty space on the strength-elongation chart, outside the classical “banana curve” displayed in figure 5.

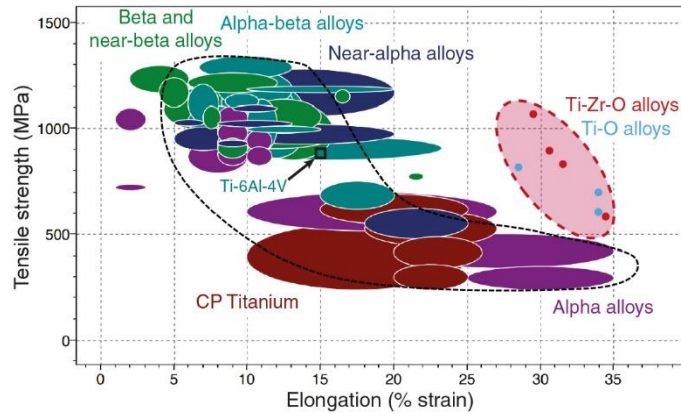


Fig. 5. Property map comparing Ti-O and Ti-Zr-O alloys with the different titanium alloy families (Data from the Cambridge Engineering Selector (CES) software).

5. Conclusion

In this work, binary Ti-O alloys with an improved combination of strength and ductility have been studied. Strengthening was attributed to the oxygen in solid solution and to recently evidenced Ti_6O -type nanoprecipitates, which also play a role in the conservation of the ductility. The main results are summarized below.

- Tensile tests highlighted a linear strengthening effect coupled with a conservation of ductility up to 0.6wt% of oxygen in Ti-O binary alloys. These trends allow the Ti-0.6O alloy to reach an improved combination of both strength and ductility, with values of 800MPa and 29%, respectively.
- Slip bands, with an intense cross-slip activity, were observed. It is proposed that the formation of these slip bands is a consequence of the interaction of the gliding dislocations with ordered Ti_6O -type precipitates by a shearing mechanism. The interaction between the dislocations in the slip bands could explain the high work-hardening rate, which has not been observed before for these amounts of oxygen. The large work-hardening rate enabled a significant homogeneous deformation and thus large elongation at fracture.

- Similarly, the ductility was maintained in oxygen-rich Ti-4.5Zr alloys displaying the same microstructure (α -phase grains with Ti₆O-type nanoprecipitates). The TiZrO alloys seem to be even more tolerant to oxygen as the Ti-4.5Zr-0.8O alloy reached a mechanical strength of 1,075MPa and 28% of elongation at fracture.

This study thus offers new possibilities for strengthening α -titanium alloys with oxygen without any loss of ductility thanks to the presence of nanoprecipitates. Further investigations concerning their formation and stability need to be performed. Their role in the deformation mechanism could then be entirely exploited to prevent the ductility loss due to oxygen.

This work also opens very promising outlooks for the use of oxygen as a full alloying element and for the development of a new generation of oxygen-strengthened titanium alloys, avoiding the use of critical alloying elements in terms of availability, safety, and biocompatibility.

Acknowledgement

Y. Millet from the Timet company is gratefully acknowledged for providing the alloys studied in this work.

Funding

The French National Research Agency (ANR) is acknowledged for the funding of TiToI Project [ANR-19-CE08-0032]. This work was also supported by the Industrial CIFRE doctoral fellowship of RP in collaboration with the company Biotech Dental.

Data availability

No data was used for the research described in the article.

Declaration of competing interest

The authors declare that they have no known competing financial interests or personal relationships that could have appeared to influence the work reported in this paper.

CRedit authorship contribution statement:

Fabienne Amann: Writing – original draft, Data curation, Conceptualization, Validation.

Régis Poulain: Writing – original draft, Conceptualization, Validation, Visualization,

Stéphanie Delannoy: Writing – review & editing. Jean-Philippe Couzinié: Writing –

review & editing. Emmanuel Clouet: Writing – review & editing. Ivan Guillot: Writing –

review & editing, Conceptualization. Frédéric Prima: Supervision, Funding Acquisition,

Writing – review & editing, Conceptualization.

6. References

- [1] D. Banerjee, J.C. Williams, Perspectives on titanium science and technology, *Acta Mater.* 61 (2013) 844–879. <https://doi.org/10.1016/j.actamat.2012.10.043>.
- [2] D. Eylon, S. Fujishiro, P.J. Postans, F.H. Froes, High-Temperature Titanium Alloys—A Review, *JOM J. Miner. Met. Mater. Soc.* 36 (1984) 55–62. <https://doi.org/10.1007/BF03338617>.
- [3] J. Gambogi, US Geological Survey, Mineral Commodity Summaries 2022 : Titanium and titanium dioxide, US Government Printing Office, Washington DC, 2022.
- [4] Z.Z. Fang, H.D. Lefler, F.H. Froes, Y. Zhang, Introduction to the development of processes for primary Ti metal production, in: *Extr. Metall. Titan. Conv. Recent Adv. Extr. Prod. Titan. Met.*, Elsevier, Amsterdam, Netherlands, 2020: pp. 1–10. <https://doi.org/10.1016/B978-0-12-817200-1.00001-6>.
- [5] R.I. Jaffee, I.E. Campbell, The Effect of Oxygen, Nitrogen, and Hydrogen on Iodide Refined Titanium, *Met. Trans.* 185 (1949) 646–654. <https://doi.org/10.1007/BF03398910>.
- [6] R.I. Jaffee, H.R. Ogden, D.J. Maykuth, Alloys of Titanium with Carbon, Oxygen, and Nitrogen, *Trans. AIME - J. Met.* 188 (1950) 1261–1266. <https://doi.org/10.1007/bf03399142>.
- [7] W.L. Finlay, J.A. Snyder, Effects of three interstitial solutes (nitrogen, oxygen, and carbon) on the mechanical properties of high-purity, alpha titanium, *Trans. AIME - J. Met.* 188 (1950) 277–286. <https://doi.org/10.1007/BF03399001>.
- [8] H. Conrad, Effect of interstitial solutes on the strength and ductility of titanium, *Prog. Mater. Sci.* 26 (1981) 123–403. [https://doi.org/10.1016/0079-6425\(81\)90001-3](https://doi.org/10.1016/0079-6425(81)90001-3).
- [9] M.L. Wasz, F.R. Brotzen, R.B. McLellan, A.J.J. Griffin, Effect of oxygen and hydrogen on mechanical properties of commercial purity titanium, *Int. Mater. Rev.* 41 (1996) 1–12. <https://doi.org/10.1179/imr.1996.41.1.1>.
- [10] Y. Chong, M. Poschmann, R. Zhang, S. Zhao, M.S. Hooshmand, E. Rothchild, D.L. Olmsted, J.W. Morris, D.C. Chrzan, M. Asta, A.M. Minor, Mechanistic basis of oxygen sensitivity in titanium, *Sci. Adv.* 6 (2020) 1–11. <https://doi.org/10.1126/sciadv.abc4060>.
- [11] G. Lutjering, J.C. Williams, *Titanium*, 2nd editio, Springer-Verlag Berlin Heidelberg, Berlin, Germany, 2007.
- [12] R.O. Ritchie, The conflicts between strength and toughness, *Nat. Mater.* 10 (2011) 817–822. <https://doi.org/10.1038/nmat3115>.

- [13] J.M. Oh, B.G. Lee, S.W. Cho, S.W. Lee, G.S. Choi, J.W. Lim, Oxygen effects on the mechanical properties and lattice strain of Ti and Ti-6Al-4V, *Met. Mater. Int.* 17 (2011) 733–736. <https://doi.org/10.1007/s12540-011-1006-2>.
- [14] B. Sun, S. Li, H. Imai, T. Mimoto, J. Umeda, K. Kondoh, Fabrication of high-strength Ti materials by in-process solid solution strengthening of oxygen via P/M methods, *Mater. Sci. Eng. A.* 563 (2013) 95–100. <https://doi.org/10.1016/j.msea.2012.11.058>.
- [15] D.S. Kang, K.J. Lee, E.P. Kwon, T. Tsuchiyama, S. Takaki, Variation of work hardening rate by oxygen contents in pure titanium alloy, *Mater. Sci. Eng. A.* 632 (2015) 120–126. <https://doi.org/10.1016/j.msea.2015.02.074>.
- [16] S.D. Luo, T. Song, S.L. Lu, B. Liu, J. Tian, M. Qian, High oxygen-content titanium and titanium alloys made from powder, *J. Alloys Compd.* 836 (2020). <https://doi.org/10.1016/j.jallcom.2020.155526>.
- [17] H. Liu, M. Niinomi, M. Nakai, X. Cong, K. Cho, C.J. Boehlert, V. Khademi, Abnormal Deformation Behavior of Oxygen-Modified β -Type Ti-29Nb-13Ta-4.6Zr Alloys for Biomedical Applications, *Metall. Mater. Trans. A Phys. Metall. Mater. Sci.* 48 (2017) 139–149. <https://doi.org/10.1007/s11661-016-3836-5>.
- [18] Q. Yu, L. Qi, T. Tsuru, R. Traylor, D. Rugg, J.W. Morris, M. Asta, D.C. Chrzan, A.M. Minor, Origin of dramatic oxygen solute strengthening effect in titanium, *Science*. 347 (2015) 635–639. <https://doi.org/10.1088/1751-8113/44/8/085201>.
- [19] S. Naka, A. Lasalmonie, P. Costa, L.P. Kubin, The low-temperature plastic deformation of α -titanium and the core structure of a-type screw dislocations, *Philos. Mag. A Phys. Condens. Matter, Struct. Defects Mech. Prop.* 57 (1988) 717–740. <https://doi.org/10.1080/01418618808209916>.
- [20] B. Barkia, J.P. Couzinié, S. Lartigue-Korinek, I. Guillot, V. Doquet, In situ TEM observations of dislocation dynamics in α titanium: Effect of the oxygen content, *Mater. Sci. Eng. A.* 703 (2017) 331–339. <https://doi.org/10.1016/j.msea.2017.07.040>.
- [21] N. Chaari, D. Rodney, E. Clouet, Oxygen-dislocation interaction in titanium from first principles, *Scr. Mater.* 162 (2019) 200–203. <https://doi.org/10.1016/j.scriptamat.2018.11.025>.
- [22] R. Poulain, S. Delannoy, I. Guillot, F. Amann, S. Lartigue-korinek, D. Thiaudière, J. Béchade, E. Clouet, F. Prima, First experimental evidence of oxygen ordering in dilute titanium – oxygen alloys, *Mater. Res. Lett.* 10 (2022) 481–487. <https://doi.org/10.1080/21663831.2022.2057202>.
- [23] K. Kondoh, M. Fukuo, S. Kariya, K. Shitara, S. Li, A. Alhazaa, J. Umeda, Quantitative strengthening evaluation of powder metallurgy Ti–Zr binary alloys with high strength and ductility, *J. Alloys Compd.* 852 (2021) 156954. <https://doi.org/10.1016/j.jallcom.2020.156954>.
- [24] Y.A. Coutinho, S.C.K. Rooney, E.J. Payton, Analysis of EBSD Grain Size Measurements Using Microstructure Simulations and a Customizable Pattern Matching Library for Grain Perimeter Estimation, *Metall. Mater. Trans. A Phys. Metall. Mater. Sci.* 48 (2017) 2375–2395. <https://doi.org/10.1007/s11661-017-4031-z>.
- [25] N. Bozzolo, N. Dewobroto, T. Grosdidier, F. Wagner, Texture evolution during grain growth in recrystallized commercially pure titanium, *Mater. Sci. Eng. A.* 397 (2005) 346–355. <https://doi.org/10.1016/j.msea.2005.02.049>.
- [26] F.J. Gil, C. Aparicio, J.A. Planell, Effect of oxygen content on grain growth kinetics of titanium, *J. Mater. Synth. Process.* 10 (2002) 263–266. <https://doi.org/10.1023/A:1023094126132>.
- [27] J.C. Williams, A.W. Sommer, P.P. Tung, The Influence of Oxygen Concentration on the Internal Stress and Dislocation Arrangements in Titanium, *Metall. Trans.* 3 (1972) 2979–2984. <https://doi.org/10.1007/bf02652870> LA - English.
- [28] A.T. Churchman, The slip modes of titanium and the effect of purity on their occurrence during tensile deformation of single crystals, *Proc. R. Soc. London. Ser. A. Math. Phys. Sci.* 226 (1954) 216–226. <https://doi.org/10.1098/rspa.1954.0250>.
- [29] F.H. Froes, Chapter 3: Principles of Alloying Titanium, in: F.H. Froes (Ed.), *Titan. Phys. Metall. Process. Appl.*, 2015: p. 51. <https://doi.org/10.31399/asm.tb.tmpa.t54480051>.
- [30] B. Predel, Ti-Zr (Titanium-Zirconium), in: *Phase Equilibria, Crystallogr. Thermodyn. Data Bin. Alloy.*, Springer, Springer-Verlag Berlin Heidelberg, Berlin, Heidelberg, Germany, 1998: pp. 1–7.
- [31] Y. Matayashi, T. Homma, Effect of Zr addition on recrystallization behavior in rolled Ti-Zr alloys, in: *TMS Annu. Meet.*, 2015: pp. 981–988. https://doi.org/10.1007/978-3-319-48127-2_119.

- [32] S. Steinemann, Metallurgie der Knochen- und Gelenkimplantate, Langenbeck's Arch. Für Chir. 349 (1979) 307–310.
- [33] L.M. Kang, C. Yang, A Review on High-Strength Titanium Alloys: Microstructure, Strengthening, and Properties, Adv. Eng. Mater. 21 (2019) 1–27. <https://doi.org/10.1002/adem.201801359>.
- [34] Y. Zhou, F. Yang, C. Chen, Y. Shao, B. Lu, T. Lu, Y. Sui, Z. Guo, Mechanical property enhancement of high-plasticity powder metallurgy titanium with a high oxygen concentration, J. Alloys Compd. 885 (2021) 161006. <https://doi.org/10.1016/j.jallcom.2021.161006>.